The 2017 World Congress on
Advances in Structural Engineering and Mechanics (ASEM17)
28 August - 1 September, 2017, Ilsan(Seoul), Korea

Keynote Paper

On the reduction methods of structural finite element models

Jeong-Ho Kim[1)], Seung-Hwan Boo[1)], Min-Han Oh[2)], *Phill-Seung Lee[1)]

[1)] *Department of Mechanical Engineering, KAIST, Daejeon 34141, Korea*
[2)] *Offshore Engineering Research Department, Hyundai Heavy Industries, Ulsan 44032, Korea*
[1)] *phillseung@kaist.edu*

ABSTRACT

In this paper, we introduce our recent studies on the reduction methods of structural finite element models, which include error estimators for the classical reduction methods, high-performance dynamic reduction methods, and the automated static condensation method. We focus on developing numerical procedures to provide significantly accurate reduced models with computational efficiency. Using several large practical engineering problems, the performance of the proposed methods are demonstrated in terms of its solution accuracy and computational efficiency. We here summarize the related formulations and numerical results published already.

1. INTRODUCTION

Model reduction methods have been widely used to reduce the degrees of freedom (DOFs) of a large finite element model. For a long time, significant efforts have been made to develop more effective reduction methods, which provide accurate reduced models with computational efficiency. In this presentation, we review the results of our previous studies on the development of reduction methods to solve large and complex structural vibration and static problems.

When a complicated structure consisting with various substructures is designed through the cooperation of different engineers, it is very expensive to deal with its finite element models, because frequent design modifications affecting the whole and component models require repeated reanalysis. The reduction methods presented here provides effective tools for such large structures (Boo et al 2016, 2017, Kim JH et al 2017).

In the following sections, we consider three different topics: an error estimator for the Craig-Bampton (CB) method (Kim JG et al 2014 and Boo et al 2016), the improved

[*1)] Associate Professor

dual Craig-Bampton (DCB) method (Kim JH et al 2017), and the automated static condensation method for local analysis of large finite element models (Boo and Oh 2017).

2. ERROR ESTIMATOR FOR THE CRAIG-BAMPTON METHOD

For the well-known Craig-Bampton method, an accurate error estimation method was proposed (Kim JG et al 2014) and it was simplified for its computational efficiency and application to error control (Boo et al 2016).

Let us consider a global finite element model partitioned into N_s substructures fixed to its boundary interface, see Fig. 1. In the original CB formulation, the transformation matrix is constructed by using only dominant substructural modes. The global displacement vector $\mathbf{u}_g$ is approximated by

$$\mathbf{u}_g \approx \bar{\mathbf{u}}_g = \bar{\bar{\mathbf{T}}}_0 \bar{\mathbf{u}} \text{ with } \bar{\bar{\mathbf{T}}}_0 = \begin{bmatrix} \boldsymbol{\Phi}_s^d & \boldsymbol{\Psi}_c \\ \mathbf{0} & \mathbf{I}_b \end{bmatrix}, \ \bar{\mathbf{u}} = \begin{bmatrix} \mathbf{q}_s^d \\ \mathbf{u}_b \end{bmatrix}, \tag{1}$$

in which $\bar{\bar{\mathbf{T}}}_0$ and $\bar{\mathbf{u}}$ are the reduced CB transformation matrix and reduced generalized coordinate vector, respectively. $\boldsymbol{\Phi}_s^d$ and $\mathbf{q}_s^d$ are the block-diagonal eigenvector matrix that consists of dominant substructural modes and corresponding generalized coordinate vector, respectively, and $\boldsymbol{\Psi}_c$ is the constraint mode matrix. The overbar ($\bar{}$) denotes the approximated quantities.

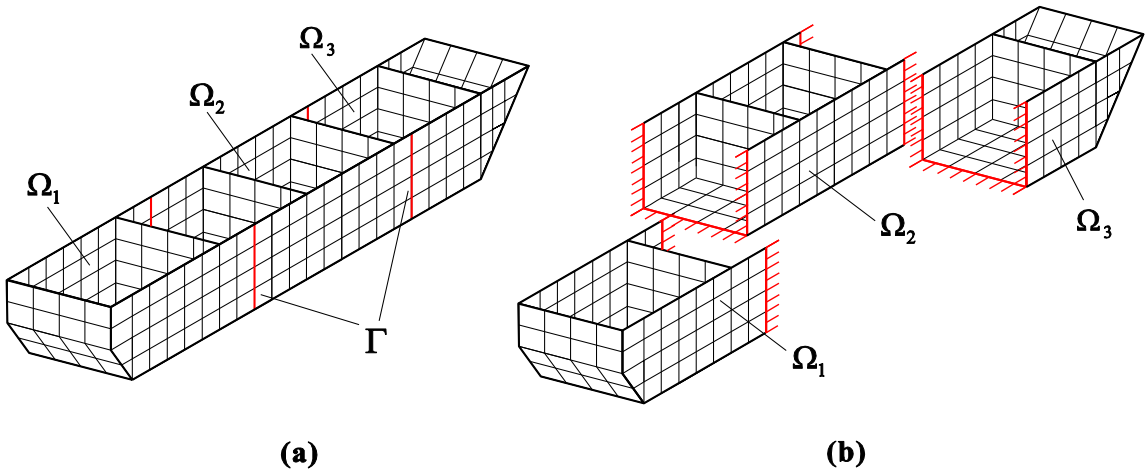

Fig. 1 Interface handling in the CB method: (a) Partitioned structure, (b) Fixed interface boundary treatment (Boo et al 2016)

The reduced matrices of the CB method could be obtained as

$$\overline{\mathbf{M}} = \overline{\mathbf{T}}_0^T \mathbf{M}_g \overline{\mathbf{T}}_0 , \ \overline{\mathbf{K}} = \overline{\mathbf{T}}_0^T \mathbf{K}_g \overline{\mathbf{T}}_0 , \tag{2}$$

where $\mathbf{M}_g$ and $\mathbf{K}_g$ are the mass and stiffness matrices of a global FE model, respectively, and then the reduced eigenvalue problem in the CB method is given by

$$\overline{\mathbf{K}}(\overline{\boldsymbol{\varphi}})_i = \overline{\lambda}_i \overline{\mathbf{M}}(\overline{\boldsymbol{\varphi}})_i \quad \text{for } i = 1, 2, \cdots, \overline{N} , \tag{3}$$

where $\overline{\lambda}_i$ and $(\overline{\boldsymbol{\varphi}})_i$ are the approximated eigenvalues and eigenvectors, respectively, and $\overline{N}$ is the number of DOFs in the reduced model.

In order to accurately estimate relative eigenvalue errors in reduced models, we construct the enhanced transformation matrix by properly considering residual substructural modes, see references; Kim JG et al 2014 and Boo et al 2016, for detailed derivations.

By using the enhanced transformation matrix $\overline{\mathbf{T}}_1$, the global displacement vector $\mathbf{u}_g$ is approximated by

$$\mathbf{u}_g \approx \overline{\mathbf{u}}_g = \overline{\mathbf{T}}_1 \overline{\mathbf{u}} \text{ with } \overline{\mathbf{T}}_1 = \overline{\mathbf{T}}_0 + \lambda \mathbf{T}_a , \tag{4}$$

in which $\overline{\mathbf{T}}_1$ is the enhanced transformation matrix, $\overline{\mathbf{T}}_0$ and $\mathbf{T}_a$ are the CB transformation matrix defined in Eq. (1), and the additional transformation matrix, respectively.

The relative eigenvalue error ξ_i could be approximated as

$$\frac{\overline{\lambda}_i}{\lambda_i} - 1 \approx \eta_i \text{ with } \eta_i = 2\overline{\boldsymbol{\varphi}}_i^T \overline{\mathbf{T}}_0^T [\overline{\lambda}_i \mathbf{M}_g - \mathbf{K}_g] \mathbf{T}_a \overline{\boldsymbol{\varphi}}_i + \overline{\boldsymbol{\varphi}}_i^T \mathbf{T}_a^T [\overline{\lambda}_i^2 \mathbf{M}_g - \overline{\lambda}_i \mathbf{K}_g] \mathbf{T}_a \overline{\boldsymbol{\varphi}}_i , \tag{5}$$

in which η_i is the original error estimator for the i-th global mode. It can be used to evaluate the accuracy of the approximated eigenvalue $\overline{\lambda}_i$ without knowing the original eigenvalue λ_i.

To investigate the performance of the new error estimator, a cargo hold structure is considered (shown in Fig. 2). Detailed specifications of the structure are described in the reference, Boo et al 2016. The number of total DOFs is 157,368, and the global structure is partitioned into 36 substructures. Two different retained substructural mode cases, $N_d = 80$ and $N_d = 290$, are considered here.

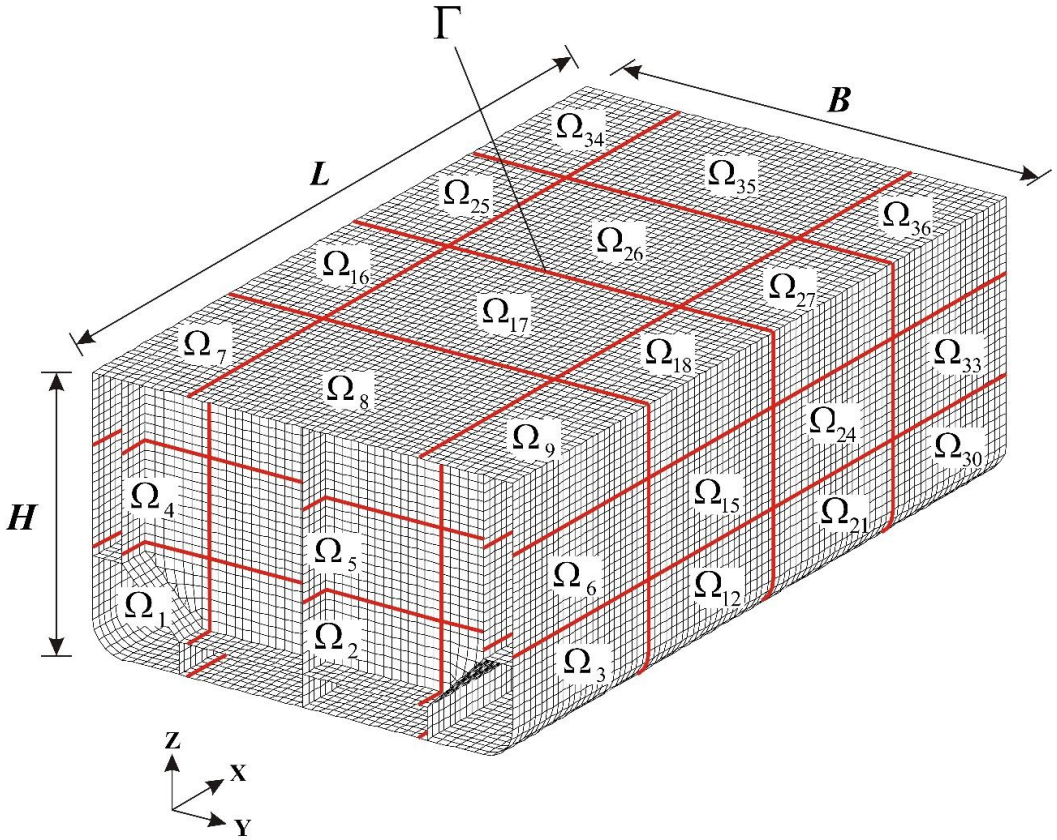

Fig. 2 Cargo hold structure problem (Boo et al 2016)

Fig. 3 shows the exact and estimated relative eigenvalue errors calculated by Eq. (5) and its simplified version (see reference, Boo et al 2016) in the two numerical cases. The estimating accuracy of the present error estimator are successfully verified.

Its estimation accuracy and computational efficiency were tested through various numerical examples in previous work. Details of the result are presented in the reference; Kim JG et al 2014 and Boo et al 2016.

3. IMPROVED DUAL CRAIG-BAMPTON METHOD

Recently, a new component mode synthesis (CMS) method was proposed by improving the DCB method (Kim JH et al 2017). The new transformation matrix was derived by considering the second order effect of residual substructural modes, and the resulting additional interface coordinates in the reduced system was eliminated by applying the concept of SEREP (the system equivalent reduction expansion process) (O'Callahan et al 1989).

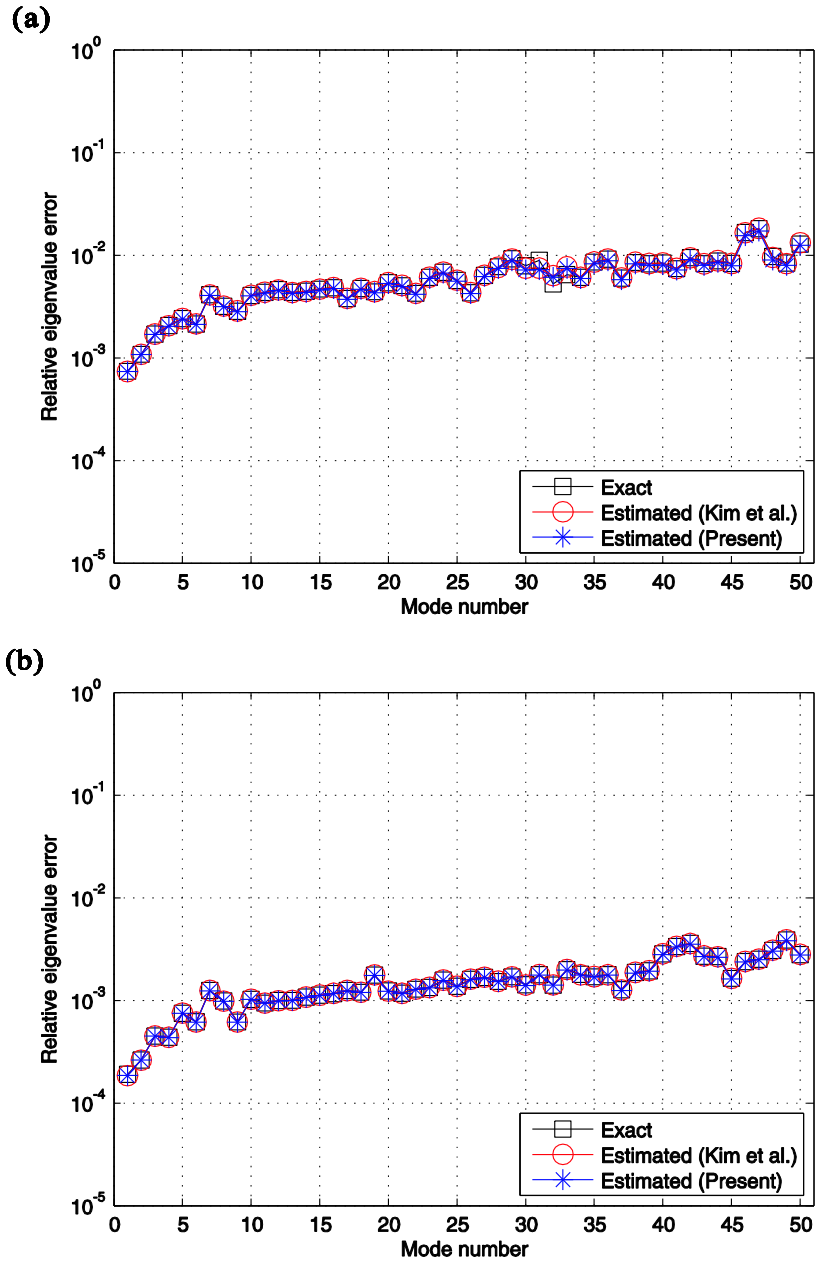

Fig. 3 Exact and estimated relative eigenvalue errors for the cargo hold structure problem: (a) $N_d = 80$, (b) $N_d = 290$ (Boo et al 2016)

In the DCB method, a structural FE model is assembled by N_s substructures as in Fig. 4a. The substructures are connected through a free interface boundary Γ (Fig. 4b). Assembling the linear dynamic equations for each substructure using explicitly defined compatibility constraint equations by using Boolean matrix $\mathbf{B}$ and Lagrange multiplier $\boldsymbol{\mu}$, the dynamic equilibrium equation of the original assembled FE model (see Fig. 4c) is constructed as

$$\begin{bmatrix} \mathbf{M} & \mathbf{0} \\ \mathbf{0} & \mathbf{0} \end{bmatrix} \begin{bmatrix} \ddot{\mathbf{u}} \\ \boldsymbol{\mu} \end{bmatrix} + \begin{bmatrix} \mathbf{K} & \mathbf{B} \\ \mathbf{B}^T & \mathbf{0} \end{bmatrix} \begin{bmatrix} \mathbf{u} \\ \boldsymbol{\mu} \end{bmatrix} = \begin{bmatrix} \mathbf{f} \\ \mathbf{0} \end{bmatrix}, \tag{6}$$

where $\mathbf{M}$ and $\mathbf{K}$ are block-diagonal mass and stiffness matrices that consist of substructural mass and stiffness matrices ($\mathbf{M}^{(i)}$ and $\mathbf{K}^{(i)}$), and $\mathbf{f}$ is the external load vector.

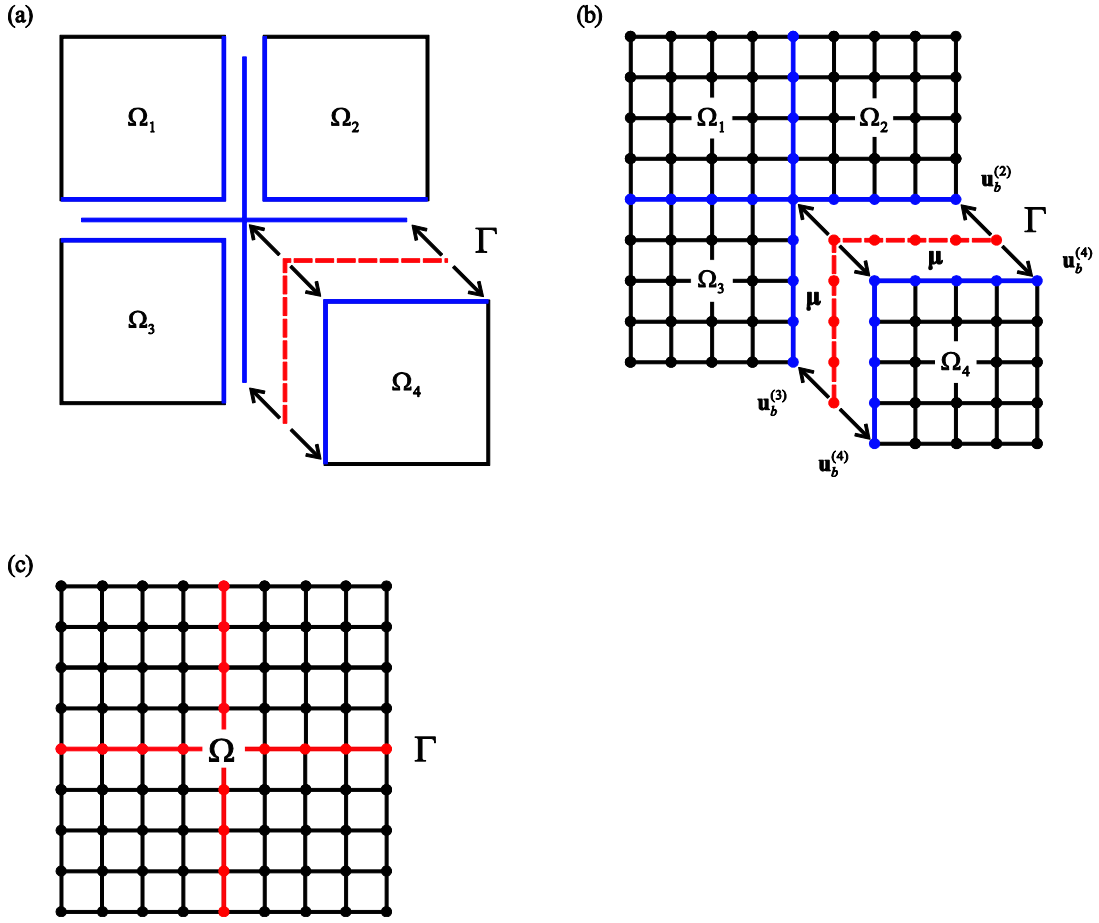

Fig. 4 Assemblage of substructures and interface handling in the DCB method ($N_s = 4$) (Kim JH et al 2017)

The displacement and Lagrange multipliers of the original assembled FE model with N_s substructures are approximated as

$$\begin{bmatrix} \mathbf{u} \\ \boldsymbol{\mu} \end{bmatrix} \approx \overline{\mathbf{T}}_2 \begin{bmatrix} \boldsymbol{\alpha} \\ \mathbf{q}_d \\ \boldsymbol{\mu} \\ \boldsymbol{\psi} \end{bmatrix} \text{ with } \overline{\mathbf{T}}_2 = \left[\begin{array}{cc|cc} \mathbf{R}_s & \boldsymbol{\Phi}_s^d & -\mathbf{F}_{rs}\mathbf{B} & -\mathbf{F}_{rm}\mathbf{B} \\ \mathbf{0} & \mathbf{0} & \mathbf{I} & \mathbf{0} \end{array}\right], \ \boldsymbol{\psi} = \lambda\boldsymbol{\mu}\,. \tag{7}$$

in which $\mathbf{R}_s$ and $\mathbf{\Phi}_s^d$ are the block-diagonal rigid body mode matrix and the matrix that consists of substructural dominant free interface normal modes, and $\boldsymbol{\alpha}$ and $\mathbf{q}_d$ are the corresponding generalized coordinate vectors. $\mathbf{F}_{rs}$ and $\mathbf{F}_{rm}$ are the matrices that consist of the substructural first and second order residual flexibility matrices, respectively.

Using the transformation matrix $\overline{\mathbf{T}}_2$ in Eq. (7), the reduced system matrices and force vector are calculated

$$\overline{\mathbf{M}} = \overline{\mathbf{T}}_2^T \begin{bmatrix} \mathbf{M} & \mathbf{0} \\ \mathbf{0} & \mathbf{0} \end{bmatrix} \overline{\mathbf{T}}_2 , \; \overline{\mathbf{K}} = \overline{\mathbf{T}}_2^T \begin{bmatrix} \mathbf{K} & \mathbf{B} \\ \mathbf{B}^T & \mathbf{0} \end{bmatrix} \overline{\mathbf{T}}_2 , \; \overline{\mathbf{f}} = \overline{\mathbf{T}}_2^T \begin{bmatrix} \mathbf{f} \\ \mathbf{0} \end{bmatrix}, \tag{8}$$

in which $\overline{\mathbf{M}}$, $\overline{\mathbf{K}}$, and $\overline{\mathbf{f}}$ are the reduced mass and stiffness matrices ($N_2 \times N_2$), and the reduced force vector ($N_2 \times 1$), respectively.

The modes related to the additional coordinates can be eliminated through a further reduction using SEREP. From the reduced system matrices in Eq. (8), the following eigenvalue problem is obtained:

$$\overline{\mathbf{K}}(\overline{\boldsymbol{\varphi}})_i = \overline{\lambda}_i \overline{\mathbf{M}}(\overline{\boldsymbol{\varphi}})_i , \; i = 1, \cdots, N_2 , \tag{9}$$

where $\overline{\lambda}_i$ and $(\overline{\boldsymbol{\varphi}})_i$ are the i -th eigenvalue and the corresponding mode vector, respectively. We then calculate the eigenvectors up to the N_1-th mode, where N_1 is the size of reduced system matrices obtained from the original DCB method.

Then, the transformation matrix of the improved DCB method is further reduced using retained eigenvectors.

$$\hat{\mathbf{T}}_2 = \overline{\mathbf{T}}_2 \overline{\mathbf{\Phi}} \text{ with } \overline{\mathbf{\Phi}} = \begin{bmatrix} (\overline{\boldsymbol{\varphi}})_1 & (\overline{\boldsymbol{\varphi}})_2 & \cdots & (\overline{\boldsymbol{\varphi}})_{N_1} \end{bmatrix} , \tag{10}$$

and thus the new transformation matrix $\hat{\mathbf{T}}_2$ has the same size as the transformation matrix in the original DCB method. That is, the additional coordinate vector $\boldsymbol{\psi}$ is eliminated.

Finally, the resulting reduced system matrices are calculated as follows:

$$\hat{\mathbf{M}} = \hat{\mathbf{T}}_2^T \begin{bmatrix} \mathbf{M} & \mathbf{0} \\ \mathbf{0} & \mathbf{0} \end{bmatrix} \hat{\mathbf{T}}_2 , \; \hat{\mathbf{K}} = \hat{\mathbf{T}}_2^T \begin{bmatrix} \mathbf{K} & \mathbf{B} \\ \mathbf{B}^T & \mathbf{0} \end{bmatrix} \hat{\mathbf{T}}_2 , \; \hat{\mathbf{f}} = \hat{\mathbf{T}}_2^T \begin{bmatrix} \mathbf{f} \\ \mathbf{0} \end{bmatrix}, \tag{11}$$

in which $\hat{\mathbf{M}}_2$, $\hat{\mathbf{K}}_2$, and $\hat{\mathbf{f}}_2$ are the final reduced mass, stiffness matrices, and force vector, respectively. Then, the size of the reduced system matrices provided by the

improved DCB method becomes equal to that by the original DCB method.

Let us consider the rectangular plate problem with a non-matching mesh case, see Fig. 5b. The whole structure is an assemblage of two substructures ($N_s = 2$). In this case, the interface compatibility is considered through nodal collocation and thus the matrices $\mathbf{B}^{(i)}$ are no longer Boolean, see Fig. 5c.

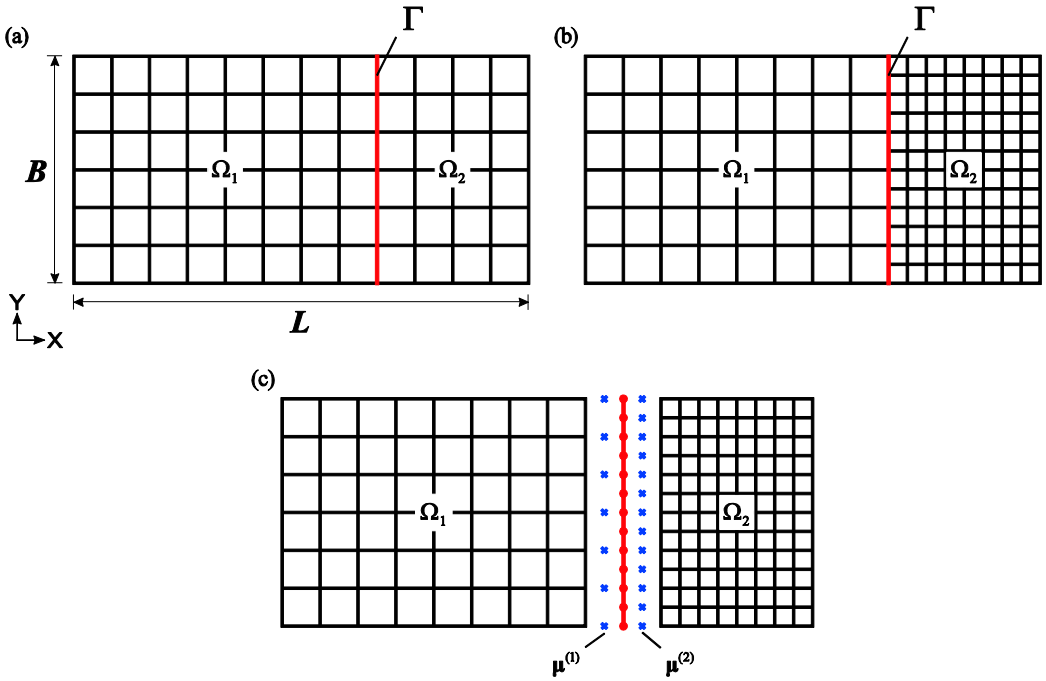

Fig. 5 Rectangular plate problem: (a) Matching mesh on the interface, (b) Non-matching mesh between neighboring substructures, (c) Interface boundary treatment (Kim JH et al 2017)

Fig. 6 presents the relative eigenfrequency errors obtained by the original and improved DCB methods. In this example, five and three dominant modes are used for each substructure in both original and improved DCB method. The results showed that the improved method provides considerably more-accurate solutions for this non-matching mesh case.

An important feature of the improved DCB method lies in the fact that the accuracy of reduced models is remarkably improved and negative eigenvalues are avoided in lower modes. In the previous work (Kim JH et al 2017), through various numerical examples, we demonstrated accuracy and computational efficiency of the improved DCB method compared to the original DCB method. Details of the results are presented in the reference, Kim JH et al 2017.

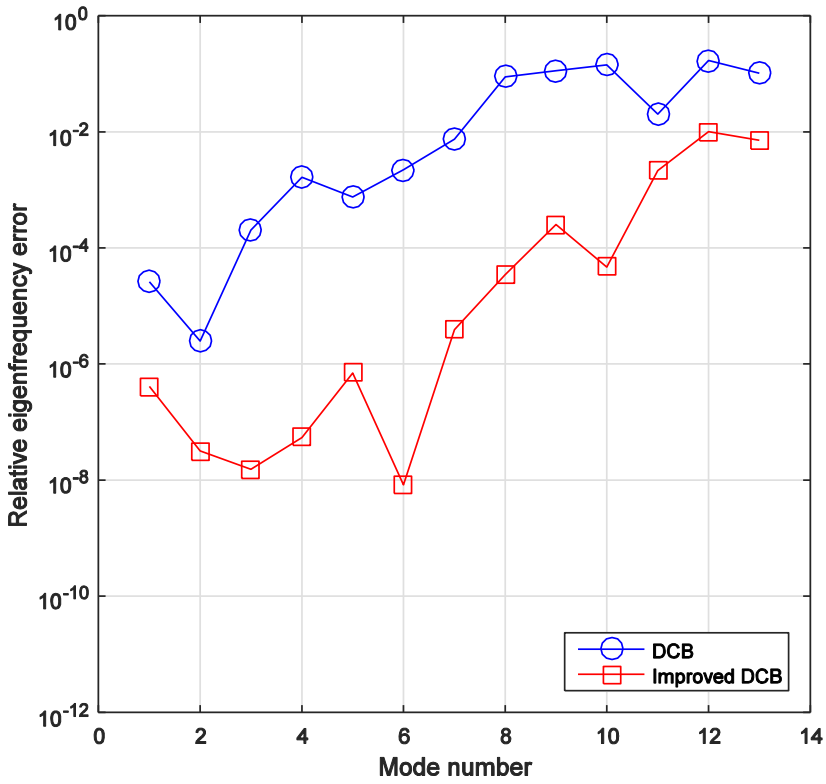

Fig. 6 Relative eigenfrequency errors in the rectangular plate problem with non-matching mesh in Fig. 7b (Kim JH et al 2017)

4. AUTOMATED STATIC CONDENSATION METHOD

We introduce an efficient new model reduction method, named the automated static condensation method, which is developed for the local analysis of large finite element models. Here, the algebraic multilevel substructuring procedure (Boo et al 2017) is modified appropriately, and then applied to the original static condensation method, see reference, Boo and Oh 2017.

In the algebraic multilevel substructuring (Karypis and Kumar 1998, Boo et al 2017), the global matrix, which is a very sparse matrix, is automatically permuted, and partitioned into many submatrices. However, the stiffness terms for the local model to be analyzed may be scattered in the permuted matrix. Fortunately, because the node numbers of the local model are already known, through the re-permutation of the matrix, the scattered stiffness terms can be gathered intentionally. Then, we can define the retained substructure, which corresponds to the local model to be analyzed. The modified algebraic multilevel substructuring procedure is shown in Fig. 7.

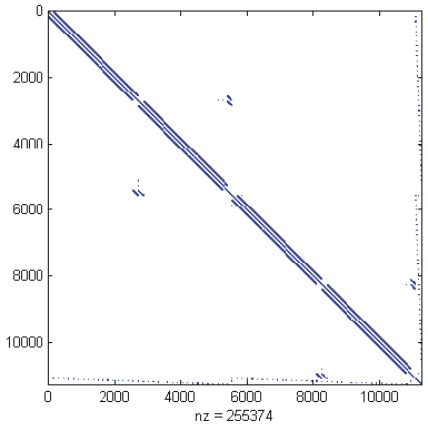

(a) Original large sparse matrix

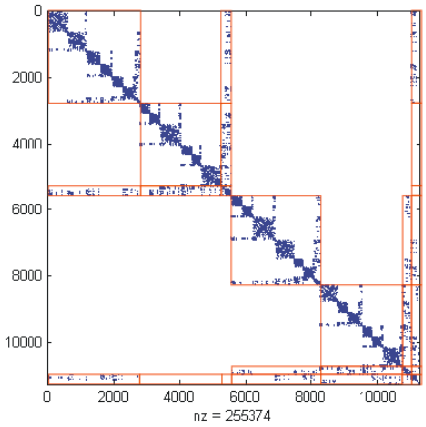

(b) Matrix permutation and partitioning

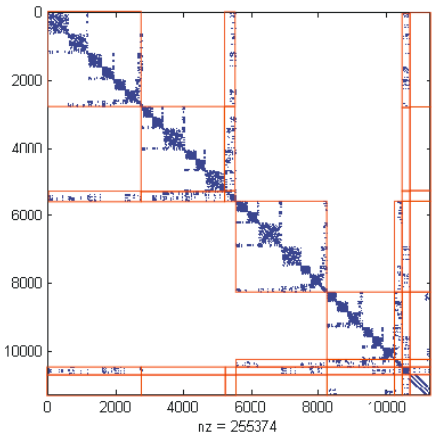

(c) Re-permutated and re-partitioned matrix

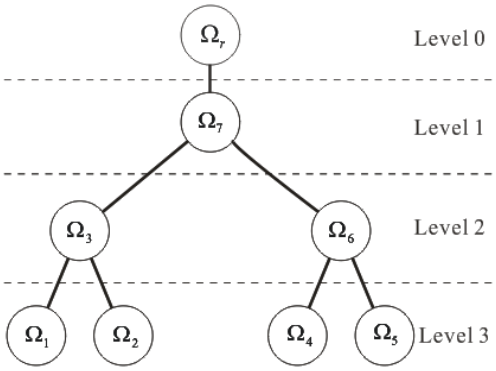

(d) Substructural tree diagram

Fig. 7 Modified Algebraic multilevel substructuring procedure (eight substructures with three substructural level, where Ω_r denotes the retained substructure to be analyzed) (Boo and Oh 2017)

The updated stiffness and force terms during the condensation procedure, and detailed derivations to construct the reduced linear static equation were described in reference, Boo and Oh 2017. The computational procedure of the automated static condensation method proposed is described in Fig. 8.

The numerical results showed that the computational efficiency of the proposed method was much superior to that of the original static condensation method with the superelement technique. Details of the results are presented in the reference, Boo and Oh 2017.

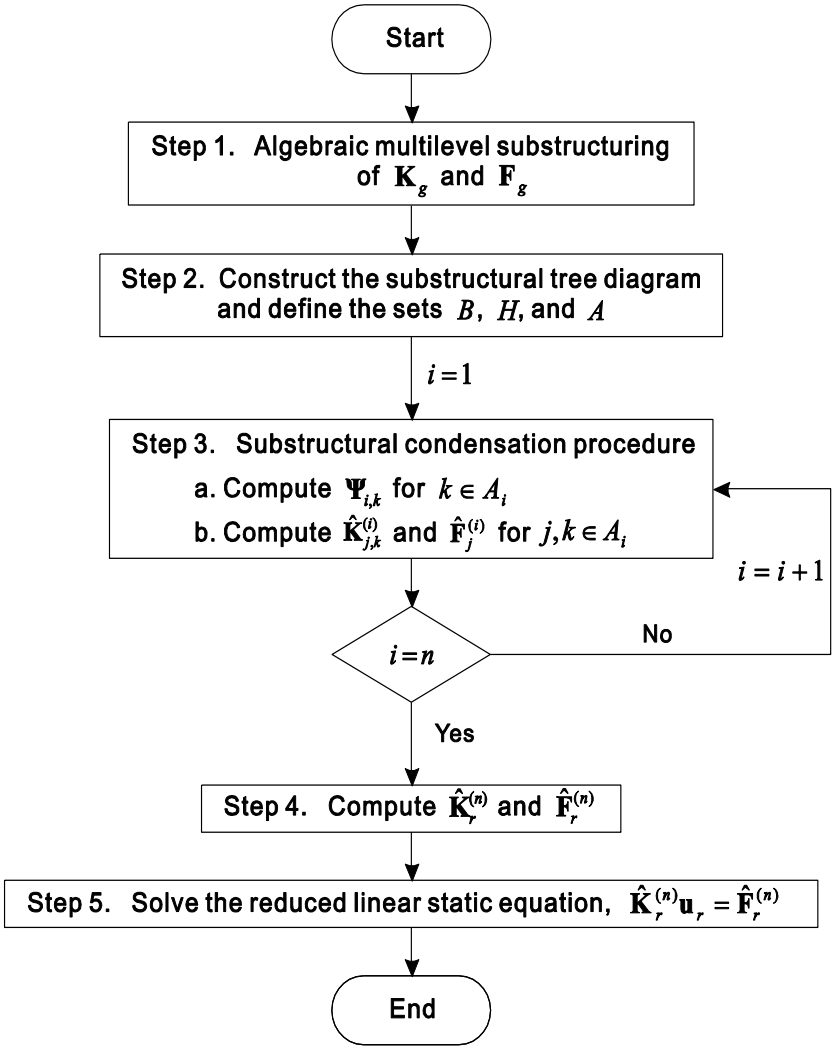

Fig. 8 Computational procedure of the automated static condensation method (Boo and Oh 2017)

5. CONCLUSIONS

In this presentation, we reviewed the formulations of the accurate error estimator and the high-performance model reduction methods recently developed. Their performances were briefly presented through representative numerical examples. We believe that the present methods will be widely utilized to analyze the behavior of large and complicated FE models in various engineering practices including efficient crash simulation techniques, structural health monitoring and experimental dynamic analyses.

ACKNOWLEDGEMENTS

This work was supported by the Basic Science Research Program through the National Research Foundation of Korea (NRF) funded by the Ministry of Science, ICT &

Future Planning (No. 2014R1A1A1A05007219), and the grant (MPSS-CG-2015-01) through the Disaster and Safety Management Institute funded by Ministry of Public Safety and Security of Korean government.

REFERENCES

Bennighof, J.K., Lehoucq, R.B. (2004), "An automated multi-level substructuring method for eigenspace computation in linear elastodynamics", *SIAM. J. Sci. Comput.*, **25**(6), 2084-106.

Boo, S.H., Kim, J.G., Lee, P.S. (2016), "A simplified error estimator for the CB method and its application to error control", *Comput. Struct.*, **164**, 53-62.

Boo, S.H., Kim, J.G., Lee, P.S. (2016), "Error estimation for the automated multi-level substructuring method", *Int. J. Numer. Meth. Eng.*, **106**(11), 927-950.

Boo, S.H., Lee, P.S. (2017), "A dynamic condensation method using algebraic substructuring", *Int. J. Numer. Meth. Eng.*, **109**(12), 1701-1720.

Boo, S.H., Oh, M.H. (2017), "Automated static condensation method for local analysis of large finite element models", *Struct. Eng. Mech.*, **61**(6), 807-816.

Boo, S.H., Lee, P.S. (2017), "An iterative algebraic dynamic condensation method and its performance", *Comput. Struct.*, **182**, 419-429.

Craig, R.R., Bampton, M.C. (1968), "Coupling of substructures for dynamic analysis", *AIAA J*, ***6***(7), 1313-1319.

Elssel, K., Voss, H. (2007), "An a priori bound for automated multi-level substructuring", *SIAM. J. Matrix. Anal. A.*, **28**(2), 386-97.

Karypis, G. and Kumar, V. (1998), "METIS v4.0, A software package for partitioning unstructured graphs, partitioning meshes, and computing fill-reducing orderings of sparse matrices", *Technical report*, University of Minnesota, Minneapolis, MN, USA.

Kim, J.G., Lee, K.H., Lee, P.S. (2014), "Estimating relative eigenvalue errors in the Craig-Bampton method", *Comput. Struct.*, **139**, 54-64.

Kim, J.G., Lee, P.S. (2014), "An accurate error estimator for Guyan reduction". *Comput. Method. Appl. M.*, **278**, 1-19.

Kim, J.G., Boo, S.H., Lee, P.S. (2015), "An enhanced AMLS method and its performance", *Comput. Method. Appl. M.*, **287**, 90-111.

Kim, J.G., Lee, P.S. (2015), "An enhanced Craig–Bampton method", *Int. J. Numer. Meth. Eng.*, **103**(2), 79-93.

Kim, J.G., Lee, P.S. (2015), "Posteriori Error Estimation Method for Flexibility-Based Component Mode Synthesis", *AIAA. J.*, **53**(10), 2828-2837.

Kim, J.G., Boo, S.H., Lee, C.O., Lee, P.S. (2016), "On the computational efficiency of the error estimator for Guyan reduction", *Comput. Method. Appl. M.*, **305**, 759-776.

Kim, J.H., Kim, J., Lee P.S. (2017), "Improving the accuracy of the dual Craig-Bampton method", *Comput. Struct.*, **191**, 22-32.

Lee, P.S., Bathe, K.J. (2004), "Development of MITC isotropic triangular shell finite elements", *Comput. Struct.*, **82**(11-12), 945-62.

Lee, Y.G., Lee, P.S., Bathe, K.J. (2014), "The MITC3+ shell finite element and its performance", *Comput. Struct.*, **138**, 12-23.

O'Callahan, J.C. (1989), "A procedure for an improved reduced system (IRS) model", *Proceedings of the 7th international modal analysis conference,* **1**, 17-21.

O'Callahan, J.C., Avitabile, P., Riemer, R. (1989), "System equivalent reduction expansion process (SEREP)", *Proceedings of the 7th international modal analysis conference*, **1**, 29-37.

Rixen, D.J. (2004), "A dual Craig–Bampton method for dynamic substructuring", *J. Comput. Appl. Math.*, ***168***(1), 383-391.